Astron. Astrophys. 325, 1070–1076 (1997)

ASTRONOMY
AND
ASTROPHYSICS

Periodic changes of the accretion geometry in the nearly-synchronous polar RX J1940.1−1025

Ralf D. Geckeler and Rüdiger Staubert

Institut für Astronomie und Astrophysik, Astronomie, Universität Tübingen, Waldhäuserstr. 64, D-72076 Tübingen, Germany

Received 19 December 1996 / Accepted 15 April 1997

Abstract. The magnetic Cataclysmic Variable (mCV) RX J1940.1–1025 belongs to the three-member subclass of polars with a slight non-synchronism ($< 2\,\%$) between the spin of the white dwarf and the orbital rotation. In these systems the accretion geometry changes periodically with phase of the beat frequency. We have now found in RX J1940.1−1025 a periodic shift in the timings of the 'troughs' in the X-ray and optical pulse profiles with beat phase. We interpret this to be due to a longitudinal displacement of the accretion region relative to the magnetic pole and to the varying angle between the field line and the white dwarf surface, caused by the asynchronous rotation. Such an effect is expected, because the accreting matter is progressively threaded by different field lines during the beat period and therefore produces a hot spot at varying positions relative to the magnetic pole.

The application of a dipole accretion model to the data of RX J1940.1−1025 yields a refined value for the spin period of 12150.40 ± 0.08 s (epoch 1994.5), with a resulting beat period of 50.0 ± 0.3 d (1994.4). The fit includes a quadratic term in $P_{\rm spin}$, leading to a value for a secular decrease of the spin period by $-(9.8 \pm 2.9) \cdot 10^{-9}$ s/s, marginally significant. This would correspond to a synchronization time scale of 100 y, comparable to the 170 y seen in V1500 Cyg.

In addition, further constraints on the accretion geometry in RX J1940.1−1025 are given.

Key words: stars: cataclysmic variables – stars: individual: RX J1940.1−1025 – stars: magnetic fields – X-rays: stars

1. Introduction

Polars are magnetic Cataclysmic Variables consisting of a Roche lobe-filling secondary and a magnetic white dwarf primary with a field strength of typically > 10 MG (e.g. Beuermann & Burwitz 1995). The strong magnetic field prevents the formation of an accretion disk and funnels the accreted matter directly onto the white dwarf photosphere near one or both of the magnetic poles, where it impacts at a velocity of several 10^3 km s^{-1}, forming a shock. In general, also because of the strong magnetic field, the white dwarf spin period and the orbital period are synchronised.

The accretion region emits hard X-ray bremsstrahlung radiation from a post shock region and a soft X-ray/EUV blackbody component from the reprocessing of hard X-rays and the thermalising of the kinetic energy of dense accretion blobs in the white dwarf photosphere (Frank et al. 1988). Optical and near infrared spectra show cyclotron emission components also originating from the post shock flow.

For synchronous polars the azimuthal angle between the magnetic axis and the line connecting the centers of the stars is generally pointing into the leading quadrant, with angles $< 50°$ (Cropper 1990), possibly caused by an equilibrium between the accretion torque and the magnetic interaction of the primary and secondary components of the system (Wu et al. 1994). The magnetic axis is not completely locked but performes oscillations with time scales of years to decades (Andronov 1987), which may explain the observed secular shifts of the accretion regions in AM Her, WW Hor and DP Leo (Bailey et al. 1993).

There is a subclass of three known polars (all with orbital periods near 3.4 h) with a slight ($< 2\,\%$) but significant non-synchronous rotation of the white dwarf consisting of RX J1940.1−1025 , V1500 Cyg (Nova Cyg 1975) and BY Cam. These objects clearly do not belong to the intermediate polars, where the spin periods of the white dwarfs are substantially shorter than the orbital periods of the binary systems (Patterson 1994). Instead they are 'classical' polars, where the white dwarf primary is presumably temporarily out of synchronization. The locking may be re-established over time scales as short as 170 y, as seen in V1500 Cyg (Schmidt et al. 1995).

In the nearly-synchronous polars the azimuthal angle of the magnetical axis relative to the secondary changes continously with phase of the beat period $P_{\rm beat}^{-1} = \mid P_{\rm spin}^{-1} - P_{\rm orb}^{-1} \mid$. The accreting matter thus follows different field lines due to the changing magnetic geometry and impacts on the white dwarf surface at different positions relative to the magnetic pole, depending on the phase of the beat cycle. We have observed this effect in RX J1940.1−1025 as a periodic shift in the timings of well defined minima (which we call 'troughs') observed in the optical and X-ray pulse profiles. The shifts have a half amplitude of

Send offprint requests to: R.D. Geckeler

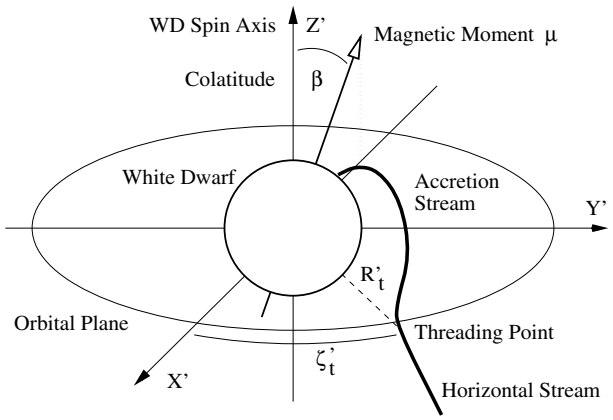

Fig. 1. Diagram of the accretion geometry in the spin system ($x'y'z'$) of the white dwarf where the z'-axis is the white dwarf spin axis. The magnetic moment $\boldsymbol{\mu}$ is inclined relative to the z'-axis by the colatitude β and is lying in the (-x')z'-plane.

$\approx$1000 s. In addition, we find evidence for a synchronization of the system on a time scale of 100 y.

2. Dipole model

In this Section we describe a dipole accretion model for nearly-synchronous polars which allows a direct comparison to the observational optical and X-ray data on RX J1940.1−1025 and the determination of the relevant physical parameters through a fitting procedure.

We have assumed a centered dipole field of the white dwarf primary, where the field lines can be described in an analytical form. We follow the coordinate conventions of Cropper (1989), with the white dwarf spin coordinate system ($x'y'z'$) and the magnetic coordinate system (xyz). Fig. 1 shows the accretion geometry in the spin system ($x'y'z'$), where the z'-axis corresponds to the white dwarf spin axis. The spin axis is assumed to be perpendicular to the orbital plane.

The magnetic moment $\boldsymbol{\mu}$ is inclined relative to the z'-axis by the colatitude β and is lying in the (-x')z'-plane. We have assumed that the infalling matter is captured in the orbital plane of the binary system at a distance $R'_{\rm t}$ from the white dwarf primary and at an azimuthal angle $\zeta'_{\rm t}$ relative to the positive x'-axis in the $x'y'$-plane.

The angle $\zeta'_{\rm t}$ rotates 360° during one beat cycle. Assuming an anticlockwise rotation of the secondary relative to the white dwarf (as seen from the positive z'-hemisphere) results in a likewise anticlockwise movement of the threading point for systems with $P_{\rm spin} > P_{\rm orb}$ and to a clockwise movement for $P_{\rm spin} < P_{\rm orb}$. For systems with $P_{\rm spin} > P_{\rm orb}$, $\zeta'_{\rm t}$ is simply defined by $\zeta'_{\rm t} = \Phi_{\rm beat} \cdot 2\pi$ and the beat phase $\Phi_{\rm beat}(T) = (T - T_0)/P_{\rm beat}$, where T_0 is the time when the threading point crosses the +x'-axis.

We have also included the effects of the varying magnetic field strength of a dipole field as a function of the angle $\epsilon_{\rm t}$ between the magnetic axis and the direction to the threading point on the threading radius. Therefore we have assumed a radial infall of the accreting matter before it is captured by the magnetic field.

The threading radius $R'_{\rm t}$ can be estimated by equating the ram pressure $\propto \rho v^2$ of the infalling accretion stream and the magnetic pressure $\propto B^2$, leading to $R'_{\rm t} \propto B^{\alpha}_{\rm pol}$, where $B_{\rm pol}$ is the polar field strength of the white dwarf and $\alpha = 4/11$ (Mukai 1988). Hameury, King & Lasota (1986) have taken into account, that the infalling plasma stream may severely distort the magnetic field. This approach leads to $\alpha = 4/7$ and estimates of $R'_{\rm t}$ which are a factor 2 smaller compared to those, obtained by equating ram and magnetic pressure.

We have defined $R'_{\rm t0}$ as the equivalent threading radius for the infalling matter, if it is captured in the equatorial plane ($\epsilon_{\rm t} = \pi/2$) of the white dwarf dipole field:

$$R'_{\rm t}(\epsilon_{\rm t}) = R'_{\rm t0}(1 + 3\cos^2(\epsilon_{\rm t}))^{\alpha/2}$$

This is a first order correction, assuming a radial infall of the accreting matter ($\epsilon_{\rm t}$=const). This approach also assumes a constant accretion rate $\dot{M}$ from the secondary. Due to the lack of detailled theoretical modelling of the magnetospherical interaction of the accreting matter, we have adopted $\alpha = 4/11$ to correct for the varying field strength.

The cartesian coordinates ($x'_{\rm tp}y'_{\rm tp}z'_{\rm tp}$) of the threading point (see Fig. 1) in the spin/orbital coordinate system are then rotated into the coordinate system of the white dwarf dipole field, where the field line is parametrised by $\zeta = const.$ and $R(\epsilon) = R_{\rm max} sin^2(\epsilon)$. $R_{\rm max}$ is the maximum distance which the field line through the threading point can reach from the dipole center and ζ is the azimuth of the threading point in the magnetic coordinate system.

The field line at which the accreting matter is captured is followed to the white dwarf surface and the coordinates of the impact point are determined. Additionally, the field vector above the accretion region is calculated and both are then rotated back into the white dwarf spin coordinate system. The basic mathematical tools like rotation matrices can be found in Cropper (1989).

During one beat phase the threading point rotates 360° in the orbital plane and the infalling matter is captured progressively by different field lines. Fig. 2 shows the resulting ellipsoidal path, hereafter called accretion ellipse, traced by the impact point around the magnetic pole. We have assumed a colatitude $\beta = 60°$ and a threading radius $R'_{\rm t0} = 10\,R_{\rm wd}$, approximating the field geometry of RX J1940.1−1025 as derived in Sect. 6.

In the magnetic system the major half axis $\delta_{\rm a}$ and the minor half axis $\delta_{\rm b}$ of the accretion ellipse are defined by:

$$\sin\delta_{\rm a} = (R'_{\rm t}/R_{\rm wd})^{-1/2}$$
$$\sin\delta_{\rm b} = (R'_{\rm t}/R_{\rm wd})^{-1/2}\cos\beta$$

The accretion ellipse is circular for colatitude $\beta = 0°$ and is flattened to a line for $\beta = 90°$.

In addition to the spot displacement on the white dwarf surface, the contribution of the inclination of the field line (and thus the accretion funnel) relative to the surface normal at the accretion spot may be important to the interpretation of data

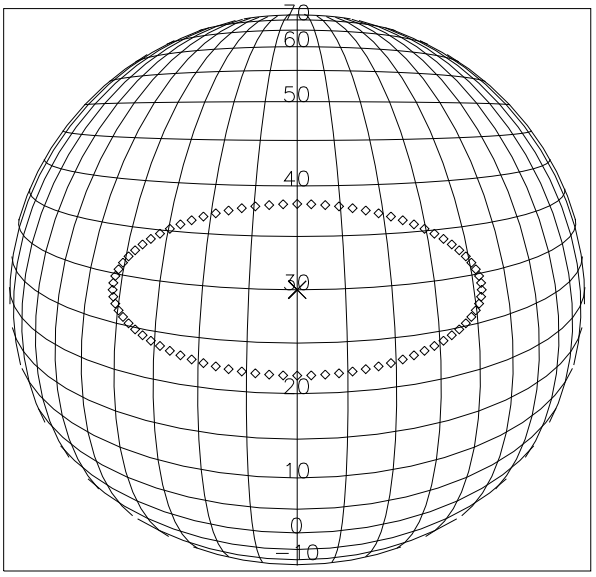

Fig. 2. Ellipsoidal path of the accretion region around the magnetic pole in a dipole field with $\beta = 60^\circ$ and $R'_{\rm t0} = 10\,R_{\rm wd}$ as seen from $0.5\,R_{\rm wd}$ above the white dwarf surface. The spacing of the coordinate grid in longitude and latitude is 5°.

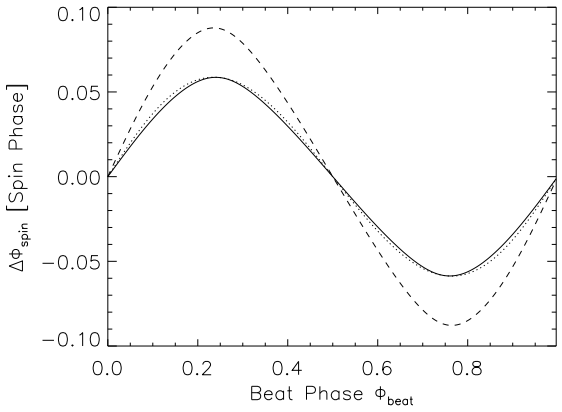

Fig. 3. Phase shift $\Delta\Phi_{\rm spin}$ between a) the time of minimum angle between the observer and the accretion funnel at the accretion spot and b) the meridian crossing of the magnetic pole as a function of beat phase $\Phi_{\rm beat}$. We have assumed $R'_{\rm t0} = 10\,R_{\rm wd}$ and $\beta = 60^\circ$. The solid line is for the assumption that the accretion funnel is perpendicular to the white dwarf surface, it also includes the correction for the varying field strength of the dipole field in the orbital plane (the dotted line excludes this correction). The dashed line shows the total phase shift including the effect of the inclination of the field lines at the white dwarf surface.

from nearly-synchronous polars. For a dipole field, the field lines at the surface are inclined (relative to the surface normal) by approximately half the angle between the magnetic axis and the line connecting the white dwarf center and the surface point. This effect has to be taken into consideration e.g. for cyclotron emission features in polars and the absorption troughs in RX J1940.1−1025, which are influenced by the field orientation, rather than the displacement of the accretion spot alone.

The displacement of the accretion region relative to the magnetic pole and the effect of the inclination of the field line in nearly-synchronous polars can therefore be detected e.g. as shifts in the timing of lightcurves and polarization features against the spin ephemeris of the system with phase $\Phi_{\rm beat}$ of the beat cycle.

Fig. 3 shows the contributions of different components to the dipole model, which will be used in the analysis of our data on RX J1940.1−1025 in Sect. 6. We have assumed $R'_{\rm t0} = 10\,R_{\rm wd}$ and $\beta = 60^\circ$, close to the best fit parameters for our object. It shows the phase shift $\Delta\Phi_{\rm spin} = (t_{\rm min} - t_{\rm pole})/P_{\rm spin}$ between a) the time $t_{\rm min}$ of minimum angle between the observer and the accretion funnel at the accretion spot and b) the meridian crossing of the magnetic pole $t_{\rm pole}$, it may be seen as phase shift relative to the spin ephemeris of the white dwarf. This phase shift varies with beat phase $\Phi_{\rm beat}$. For the solid line we have excluded the effect of the inclination of the field lines guiding the stream assuming that the accretion funnel is perpendicular to the white dwarf surface. The phase shift is then only caused by the displacement of the accretion spot from the magnetic pole, as shown in Fig. 2. If the variation of the dipole field strength in the orbital plane is neglected the dotted line results.

The dashed line shows the total phase shift including the effect of the inclination of the field lines relative to the surface normal. There are two contributions to the total phase shift: 1) due to the longitudinal displacement of the hot spot on the white dwarf surface (solid line) and 2) due to the changing orientation of the field lines guiding the accretion stream. The first contribution is about 2/3, the latter about 1/3 of the total effect.

We do not consider here the case of pole switching since, because of the geometry in RX J1940.1−1025 (i$\approx \beta$), we observe the effects of variable accretion from one pole only. Pole switching would lead to a significantly different behaviour of the longitudinal displacement as a function of beat phase during half of the beat period.

In the following Section we will discuss the general effects expected due to the varying accretion geometry in nearly-synchronous polars. To facilitate the discussion, we will assume the effects of the spot displacement only.

3. General results

The displacement of the accretion region relative to the magnetic axis of the white dwarf dipole field leads to several effects, which are of relevance to the interpretation of observational data of nearly-synchronous polars. In the following discussion we assume a nearly-synchronous system with $P_{\rm spin} > P_{\rm orb}$, as valid for RX J1940.1−1025.

The critical colatitude $\beta_{\rm crit}$ is defined by $\tan\beta_{\rm crit} = (R'_{\rm t}/R_{\rm wd})^{-1/2}$, separating accretion geometries in which the white dwarf spin axis is located outside the accretion ellipse (Case I - $\beta > \beta_{\rm crit}$) or inside of it (Case II - $\beta < \beta_{\rm crit}$). We will discuss them in turn in order to highlight the different effects associated with both geometries.

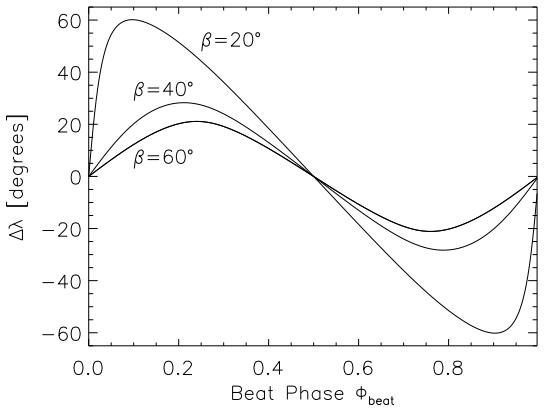

Fig. 4. Longitudinal displacement $\Delta\lambda = \lambda_{\rm spot} - \lambda_{\rm pole}$ of the accretion region from the magnetic pole (in the spin coordinate system of the white dwarf, see text) as a function of the beat phase $\Phi_{\rm beat}$, assuming $R'_{\rm t0} = 10\,R_{\rm wd}$ and three different colatitudes $\beta > \beta_{\rm crit}$.

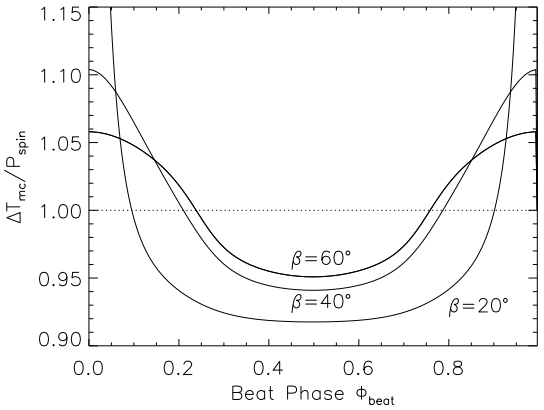

Fig. 5. The time $\Delta T_{\rm mc}/P_{\rm spin}$ between two sucessive meridian crossings of the accretion region as a function of the beat phase $\Phi_{\rm beat}$ for three colatitudes $\beta > \beta_{\rm crit}$, assuming $\Delta P/P_{\rm orb} = (P_{\rm spin} - P_{\rm orb})/P_{\rm orb} = 2.8 \cdot 10^{-3}$.

Case I: $\beta > \beta_{\rm crit}$. Accretion ellipse does not include the white dwarf spin axis.

Fig. 4 shows the observed longitudinal displacement $\Delta\lambda = \lambda_{\rm spot} - \lambda_{\rm pole}$ of the accretion spot from the magnetic pole in the spin coordinate system, assuming $R'_{\rm t0} = 10\,R_{\rm wd}$ and colatitudes β ranging from 20° to 60° in steps of 20°.

The longitudinal/latitudinal spin coordinates on the white dwarf surface have been defined according to the coordinate system on the earth, with longitudes $\lambda > 0°$ ($\lambda < 0°$) running in western (eastern) direction and the positive z′-axis defining north. Positive values for $\Delta\lambda$ thus correspond to an accretion region with a longitudinal displacement from the dipole axis in clockwise direction (as seen from the hemisphere of the positive z′-axis), with the accretion region crossing the meridian to the observer after the magnetic pole (for $P_{\rm spin} > P_{\rm orb}$).

If the accretion ellipse is located closer to the white dwarf spin axis (β approaching $\beta_{\rm crit}$), the spot displacement in the magnetic system translates into a larger longitudinal displacement in spin coordinates. The resulting graph of the displacement as a function of $\Phi_{\rm beat}$ becomes noticeably asymmetrical as the colatitude β approaches $\beta_{\rm crit}$, because parts of the accretion ellipse are located substantially closer to the converging longitudinal coordinate lines near the white dwarf spin pole during half of the beat cycle.

The movement of the accretion region complicates the determination of the white dwarf spin period since the separation $\Delta T_{\rm mc}$ between two sucessive meridian crossings of the accretion region can deviate substantially from $P_{\rm spin}$. $\Delta T_{\rm mc}$ is rather a function of beat phase. Although the mean period between sucessive meridian crossings, when sampled evenly over the beat cycle, equals the white dwarf spin period, observations over time spans short compared to the beat period $P_{\rm beat}$ of the system may lead to incorrect estimates of $P_{\rm spin}$. Results obtained with traditional period analysis tools using folding techniques and Fourier transforms must be taken with caution, because of the dependence of $\Delta T_{\rm mc}$ on $\Phi_{\rm beat}$. Fig. 5 shows the separation $\Delta T_{\rm mc}$ between two sucessive meridian crossings in units of $P_{\rm spin}$ as a function of the beat phase $\Phi_{\rm beat}$ for the parameters of Fig. 4. We have assumed $\Delta P/P_{\rm orb} = (P_{\rm spin} - P_{\rm orb})/P_{\rm orb} = 2.8 \cdot 10^{-3}$ for the graph, as valid for RX J1940.1−1025.

Case II: $\beta < \beta_{\rm crit}$. Accretion ellipse includes the white dwarf spin axis.

A different picture emerges, when the white dwarf spin axis is located inside the ellipsoidal path traced by the accretion region. The mean period between sucessive meridian crossings (when sampled evenly over the beat cycle) now equals the orbital period $P_{\rm orb}$ of the system, independent of the white dwarf spin period. The asynchronous rotation of the white dwarf primary in nearly-synchronous polars with $\beta < \beta_{\rm crit}$ may thus not be obvious when comparing spectroscopic and photometric data sets.

Fig. 6 shows the separation $\Delta T_{\rm mc}$ between two sucessive meridian crossings of the accretion region relative to the observer as a function of the beat phase for colatitudes $\beta < \beta_{\rm crit}$, assuming $R'_{\rm t0} = 10\,R_{\rm wd}$ and $\Delta P/P_{\rm spin} = 2.8 \cdot 10^{-3}$.

4. RX J1940.1−1025

Through observations with *ROSAT*, RX J1940.1−1025 has been identified as the source of the periodically modulated X-ray flux (Madejski et al. 1993, Staubert et al. 1994) which had earlier been associated with the Active Galaxy NGC 6814. RX J1940.1−1025 has been shown to be a nearly-synchronous polar (Staubert et al. 1994, Friedrich et al. 1996, Staubert et al. 1995).

The asynchronism in RX J1940.1−1025 reveals itself through strong modulations of the optical and the X-ray flux, as well as through the radial velocities of its emission lines, which follow different periods. Sharp dips (and the radial velocities) define the orbital period (12116.3 s) and a broader photometric modulation (eclipse-like 'troughs' in X-ray and optical pulse profiles) interpreted as due to the changing aspect of the accretion spot on the surface of the white dwarf determine its spin

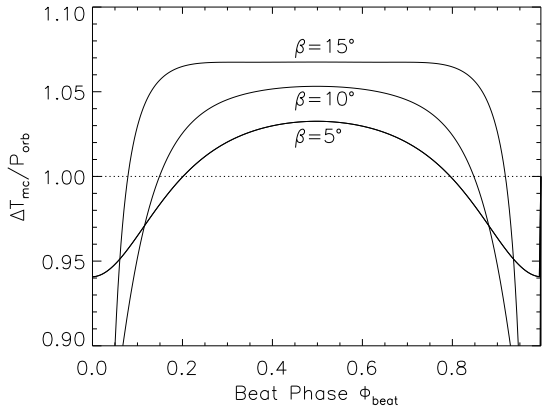

Fig. 6. Time $\Delta T_{\rm mc}/P_{\rm orb}$ between sucessive meridian crossings of the accretion spot as a function of the beat phase $\Phi_{\rm beat}$ for colatitudes $\beta < \beta_{\rm crit}$ and $R'_{\rm t0} = 10\,R_{\rm wd}$, assuming $\Delta P/P_{\rm spin} = (P_{\rm spin} - P_{\rm orb})/P_{\rm spin} = 2.8 \cdot 10^{-3}$.

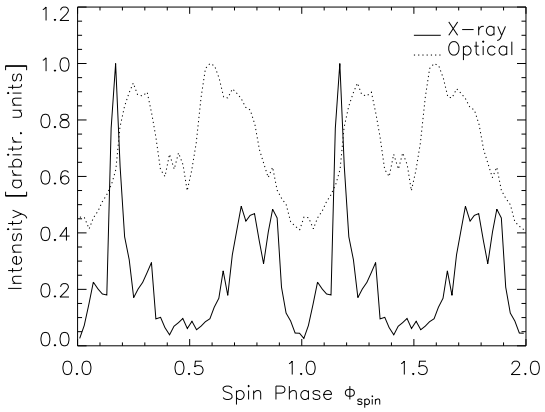

Fig. 7. Optical and X-ray pulse profiles of RX J1940.1−1025, folded with the white dwarf spin period $P_{\rm spin}$ = 12150.4 s (see text). Spin Phase 0.0 corresponds to HJD 2 449 549.7361. The well defined minimum at phase 1.0 we call 'trough'.

period (12150.4 s). The resulting beat period between the orbital and the spin period is 50.0 d.

Of the three known nearly-synchronous polars RX J1940.1−1025 has the smallest separation (0.28%) between the orbital period and the spin period and, contrary to the two others, the orbital period of RX J1940.1−1025 is the shorter one, which places an interesting theoretical problem and is not yet understood.

5. Observational results

Fig. 7 shows X-ray and optical pulse profiles of RX J1940.1−1025. The data have been corrected for the shifts according to the best fit dipole model and the quadratic component of the spin ephemeris from Sect. 7 and have then been folded with the white dwarf spin period $P_{\rm spin}$ = 12150.4 s. The X-ray data are approx. 100 ksec of ROSAT PSPC data in the energy band 0.1–2.4 keV from April 92 to October 93, the optical data are the results of our white light photometry, performed in Tübingen with the 30cm refractor and the 40cm reflector employing a CCD camera (see Friedrich et al. 1996).

Both pulse profiles can be explained in the framework of magnetic CV's by the different emission characteristics of the optical and X-ray radiation and the model of RX J1940.1−1025 we have developed in Staubert et al. (1995) and Friedrich et al. (1996).

The double peak structure of the X-ray pulse profile can be explained by the rising X-ray flux as the accretion spot is viewed more face on by the observer, with an absorption by the accretion funnel directly above the white dwarf surface cutting into the intensity peak (when the observer looks nearly parallel to the field lines above the accretion region, Imamura & Durisen 1983). This X-ray absorption trough (phase zero in the X-ray pulse profile) corresponds to a trough in the optical pulse profile. This interpretation of the pulse profiles is supported by the fact, that the peaks seen in the optical light variations of our photometric data occur prior to and after the double peak structure in the X-rays, as expected from cyclotron emission characteristics. The optical cyclotron radiation is mainly emitted perpendicular to the magnetic field and thus reaches its maximum at phases 0.2 and 0.6, when the viewing angle to the magnetic field is at a maximum and the accretion spot itself presents a small projected X-ray emitting area to the observer.

We have extracted the timings of the troughs from our extended optical photometry as well as from all available ROSAT X-ray data. Also included are photometric data sets from Patterson et al. (1995) and Watson et al. (1995). For these the published light curves were scanned and analysed in the same way as our original data. The times given in Table 1 are our best estimates for the symmetry centers of the troughs. These times were determined by superposing a mirror image and shifting it until a satisfying overlap, as found by eye, was achieved. This method was found to be more reliable than a formal best fit. The associated uncertainties are conservative estimates, typically of the order of 13% of the FWHI (full width at half intensity).

6. Application of model to RX J1940.1−1025

The mean photometric period, differing from the spectroscopic (orbital) period by 34 s, can be identified with the white dwarf spin period. According to the dipole model, the white dwarfs spin axis in RX J1940.1−1025 is outside the accretion ellipse ($\beta > \beta_{\rm crit}$).

The timings of the X-ray and optical troughs of RX J1940.1−1025 have been analyzed by simultaneously fitting a linear and quadratic spin ephemeris plus the accretion model according to Sect. 3. For the fit the orbital period has been fixed to $P_{\rm orb}$ = 0.14023495 d (Patterson et al. 1995). The trough occurs when the viewing angle between the accretion funnel above the accretion region and the direction to the observer is at a minimum. The troughs are always associated with the same pole, the one facing the observer. There are two contributions to the total time shifts, as described in Sect. 2: the first is due to the longitudinal displacement of the hot spot on

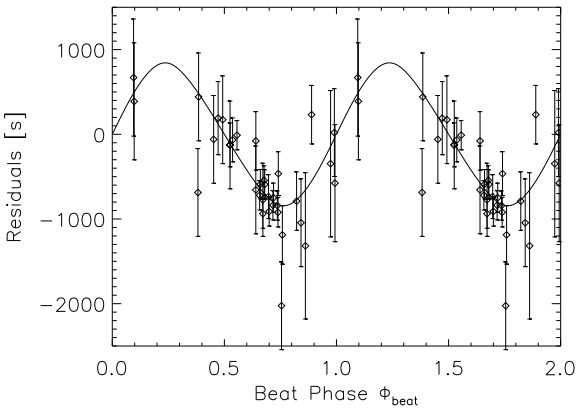

Fig. 8. Residuals of the troughs in RX J1940.1−1025 (optical plus X-ray data, see text), folded with the beat period $P_{\rm beat}$. The solid line is the best fit dipole model. (The same data are repeated for a second beat period).

Table 1. Times of the centers of the 'troughs'

Time[a]	±	Source[b]	Time	±	Source
8921.5286	0.003	X1	9577.8552	0.002	O2
8921.5286	0.006	X1	9578.6995	0.002	O2
9078.7491	0.002	X1	9578.8396	0.002	O2
9078.7510	0.005	X1	9579.6817	0.003	O2
9239.5066	0.004	O3	9579.8203	0.002	O2
9277.0452	0.006	X1	9580.6649	0.002	O2
9277.0519	0.004	X1	9580.8066	0.002	O2
9519.5027	0.006	O1	9581.6493	0.002	O2
9543.5444	0.010	O1	9581.7890	0.002	O2
9544.3925	0.006	O1	9582.7703	0.004	O2
9544.5262	0.008	O1	9632.5433	0.006	X1
9549.6033	0.008	O2	9863.7506	0.006	O1
9549.7407	0.008	O2	9863.9043	0.006	O1
9567.4548	0.006	O1	10281.4078	0.003	O1
9568.4421	0.005	O1	10285.4821	0.004	O1
9571.6736	0.003	O2	10286.4635	0.006	O1
9572.6586	0.002	O2	10287.4447	0.010	O1
9577.7131	0.002	O2			

a: HJD-2 440 000

b: X/O denotes X-ray and optical troughs. Data sources are (1) Our work, (2) Patterson et al. (1995), (3) Watson et al. (1995).

the white dwarf surface, and the second is due to the changing orientation of the field lines guiding the accretion stream (which is responsible for blocking our view of the hot spot).

Fig. 8 shows the residuals of the troughs (optical plus X-ray data from 1993-96) from the linear plus quadratic spin ephemeris from Table 2 versus beat phase $\Phi_{\rm beat}$. The data points reasonably follow the solid line which represents the best fit dipole model. The reduced chi-square $\chi^2_{\rm red}$ = 1.02 (χ^2 = 29.7 with 29 degrees of freedom = 35 data points minus 6 free parameters) of the fit shows that our estimates of the observational uncertainties of the trough timings are reasonable.

We conclude that the dipole accretion model provides a valid description of the data over the three year time span. Table 2 shows the best fit values of the free parameters for a simultaneous fit, together with their jointly estimated 1σ uncertainties ($\chi^2_{\rm min}$+7.01 for six free parameters).

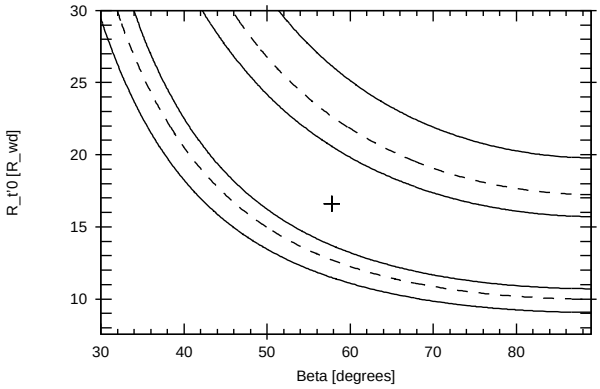

Fig. 9. χ^2 grid for the parameters β and $R'_{\rm t0}$ with contour lines for 68%, 90% and 99% confidence ($\chi^2_{\rm min}$+2.28, 4.61 and 9.21 for two free parameters). The $\chi^2_{\rm min}$ position is marked by a cross.

Table 2. Best fit parameters

Parameter	Best Fit	+1 σ	-1 σ
$R'_{\rm t0}$ $[R_{\rm wd}]$	16.6	-	-10.0
β $[degrees]$	58	-	-
$P_{\rm spin}$ $[d]$	0.14062958	$+9.4\cdot10^{-7}$	$-8.9\cdot10^{-7}$
$\dot{P}_{\rm spin}$ [s/s]	$-9.8\cdot10^{-9}$	$+2.7\cdot10^{-9}$	$-2.9\cdot10^{-9}$
$T_{\rm 0spin}$ $[HJD]$	2 449 549.7361	$+4.0\cdot10^{-3}$	$-4.1\cdot10^{-3}$
$T_{\rm 0beat}$ $[HJD]$	2 449 494.9	+4.1	-3.3

The data yield a refinement of the white dwarf spin period $P_{\rm spin}$ = 12150.40 ± 0.08 s, with a resulting beat period of $P_{\rm beat}$ = 50.0 ± 0.3 d (for epochs 1994.5 and 1994.4, respectively).

The fitting of the model to the data allows to give a tight constraint on the combined parameter $(R'_{\rm t0}/R_{\rm wd})^{1/2}\sin\beta$ = 3.47 ± 0.15 (for $\beta > 35°$). The parameters $R'_{\rm t0}$ and β are not well constrained individually (as can be seen in the large or not defined $\pm1\sigma$ errors in Table 2), because an increase in the colatitude β can be compensated for by an increase in the size of the accretion ellipse and thus a decrease in $R'_{\rm t0}$ (for a given amplitude of the observed shifts). This purely geometrical relationship between those two parameters can be expressed as $(R'_{\rm t0}/R_{\rm wd})^{1/2}\sin\beta = const.$ and results in graphs of $\Delta\lambda$ as a function of $\Phi_{\rm beat}$ with almost identical shape and amplitude over a wide range of colatitudes with $\beta > 35°$.

To demonstrate this effect, the resulting elongated valley in χ^2 as a function of $R'_{\rm t0}$ and β is illustrated in Fig. 9. The contour lines are for 68%, 90% and 99% confidence levels ($\chi^2_{\rm min}$+2.28, 4.61 and 9.21 for two free parameters). The $\chi^2_{\rm min}$ position is marked by a cross. To emphasize the $(R'_{\rm t0}/R_{\rm wd})^{1/2}\sin\beta$-relationship, the other parameters of the model are fixed to their best fit values. This χ^2 valley is narrower compared to the one resulting from a fit, where all 6 parameters are set free (as used in the determination of the best fit parameters).

The fit with all parameters set free (Table 2) results in $R'_{t0} > 6.6\,R_{wd}$ at the 68% confidence level. Together with an estimate of R'_{t0} from Mukai 1988 and of the accretion rate from the P_{orb}-$\dot{M}$- relation ($\dot{M} \propto P_{orb}^{3.2}$) of Patterson (1984) ($\dot{M} = 2 \cdot 10^{16}$ g s^{-1}), this results in $B_{pol} > 10^7$ G for the white dwarf, as expected for a polar.

In the spin ephemeris we have included a quadratic term to account for a possible spin period derivative $\dot{P}_{spin}$. The combined fit to the X-ray and optical data is significantly degraded by using a linear ephemeris only, with the χ^2 increasing from 29.7 to 121.6. An F-test reveals a probability $< 0.5\%$ that the improvement of the fit to the data due to the quadratic component is purely by chance and not due to a better description of the data by the model. The best fit value for the quadratic term of the fit corresponds to a secular decrease of the white dwarf spin period of $\dot{P}_{spin} = -9.8 \cdot 10^{-9}$ s/s. The formal uncertainty of this value when fitting six free parameters simultaneously is $2.9 \cdot 10^{-9}$ s/s (χ^2_{min}+7.01).

We have also checked, whether a shift between the X-ray and optical troughs due to different locations of the emission regions on the white dwarf surface exists. X-ray and optical data are not evenly spread over the time span during which RX J1940.1−1025 has been observed. Therefore a systematic shift may introduce a spurious $\dot{P}_{spin}$ in the fit. Such a systematic shift would be expected if material responsible for the optical and X-ray emissions did couple at different threading points (e.g in azimuth). We have simultaneously fitted a linear spin ephemeris, plus the dipole accretion model, which allows for the above shift. This results in a fit with $\chi^2 = 77.2$ (as compared to $\chi^2 = 29.7$ for the fit with the quadratic term) and a shift of the X-ray threading azimuth of $70 \pm 39^\circ$ relative to that of the optical azimuth.

We prefer the interpretation that there is evidence for a $\dot{P}_{spin}$ of the order of -10^{-8} s/s, with a resulting synchronization time scale of 100 y, comparable to the 170 y seen in V1500 Cyg, although a fit to the optical data alone, which cover a shorter time span (2.9 y) as compared to the combined data set (3.7 y), results in no significant $\dot{P}_{spin}$.

7. Summary

We have observed the effects of the varying accretion geometry between the infalling accretion stream and the magnetic field of the white dwarf primary in the nearly-synchronous polar RX J1940.1−1025. The data can be explained with a dipole field configuration. There is evidence for a secular decrease of the spin period of RX J1940.1−1025 with a synchronization time scale of the order of 100 y. Further data will be necessary to pin down an exact value for the synchronization time scale, which will allow to gain insight into the accretion and synchronization torques at work in the nearly-synchronous systems and the magnetic CV's in general.

We note that systematic studies of nearly-synchronous polars extending over at least one beat period provide a unique opportunity to gain insight into the not well understood interaction between the infalling accretion stream and the white dwarf magnetosphere. Extended photometry, polarimetry and X-ray observations would allow to study the varying field geometry above the accretion region and the location of the accretion spot to determine the magnetic field configurations of the white dwarf primaries.

A model for nearly-synchronous systems does not only have to explain the observational facts of one orbital/spin cycle, but must hold for the whole beat cycle. This leads to constraints on model parameters, which are not present in the case of locked polars.

Acknowledgements. This work was supported by DARA under grant 50 OR 96031 and by DFG under grant ST 173/22-1. We acknowledge significant contributions to the Tübingen CCD photometry by G. Lamer, S. Friedrich and M. König, as well as further optical data from E. Paunzen, Wien. For the model fitting and the calculation of confidence contours the routine DOFIT developed by F. Rother has been used. We thank the anonymous referee for useful comments on this paper.

References

Andronov, I.L., 1987, Astrophys.Space Sci., 131, 557
Bailey, J., Wickramasinghe, D.T., Ferrario, L. et al. 1993, MNRAS, 261, L31
Beuermann, K., Burwitz, V. 1996, In: Proc. Cape Workshop on Magnetic CVs, p. 99, Eds. Buckley, D.A.H. and Warner, B. ASP Conf. Series 85
Cropper, M. 1989, MNRAS, 236, 935
Cropper, M. 1990, Space Science Reviews, 54, 195
Frank, J., King, A.R., Lasota J.P., 1988, A&A, 193, 113
Friedrich, S., Staubert, R., Lamer, G. et al. 1996, A&A, 306, 860
Hameury, J.-M., King, A.R., Lasota, J.-P. 1986, MNRAS, 218, 695
Imamura, J.N.,Durisen, R.H. 1983, ApJ, 268, 291
Li, J., Wickramasinghe, D.T., Wu, K. 1995, MNRAS 276, 255
Liebert, J., Stockman, H.S. 1985, In: CV's and LMXB's, p.151,Eds. Lamb, D.Q. and Patterson, J., Reidel, Dordrecht
Lubow, S.H., Shu, F.H., 1975, Ap.J., 198, 383
Madejski, G.M., Done, C., Turner, T.J., et al. 1993, Nat, 365, 626
Meyer, F., Meyer-Hofmeister, E., 1983, A&A, 121, 29
Mukai, K. 1988, MNRAS, 232, 175
Patterson, J. 1984, ApJS, 54, 443
Patterson, J. 1994, PASP, 106, 209
Patterson, J., Skillman, D.R., Thorstensen, J., et al. 1995, PASP, 107, 307
Ritter, H. 1986, In: The Evolution of Galactic XRB's, p. 271, Eds.Trümper, J., et al., Reider, Dordrecht
No. 5850
Schmidt, G.D., Liebert, J., Stockman, H.S. 1995, ApJ 441, 414
Schwope, A.D., Schwarz, R., Mantel, K.-H. et al. 1996, In: Proc. Cape Workshop on Magnetic CVs, p. 166, Eds. Buckley, D.A.H. and Warner, B. ASP Conf. Series 85
Staubert, R., König, M., Friedrich, S., et al. 1994, A&A, 288, 513
Staubert, R., Friedrich, S., Lamer, G., et al. 1995, In: Proc. Cape Workshop on Magnetic CVs, p. 264, Eds. Buckley, D.A.H. and Warner, B. ASP Conf. Series 85
Watson, M.G., Rosen, S.R., O'Donoghue, D., et al. 1995, MNRAS, 273, 681
Wu, K., Wickramasinghe, D.T., Bailey, J. et al. 1994, Proc.ASA, 11(2), 198